View Online

Green synthesis of tunable $Cu(In_{1-x}Ga_x)Se_2$ nanoparticles using non-organic solvents

Layla Al Juhaiman,[a,b] Ludmila Scoles,[a] David Kingston,[a] Bussaraporn Patarachao,[a] Dashan Wang[a] and Farid Bensebaa*[a]

Received 28th January 2010, Accepted 29th April 2010
First published as an Advance Article on the web 27th May 2010
DOI: 10.1039/c001813a

A green synthesis route of $Cu(In_{1-x}Ga_x)Se_2$ nanoparticles with variable Ga content is described in this report for the first time. Only water and a minimum amount of energy input are used. Heating appropriate amounts of Cu, In, Ga and Se dispersed in an aqueous solution containing mercapto-acetic acid in a microwave oven gives rise to small and uniform nanoparticles. These new materials have been characterized to confirm composition, geometrical and structural properties. Transmission electron microcopy (TEM) confirmed size distribution around 4 nm. XRD confirmed the chalcopyrite structure with an average crystallite size of 3 nm. Atomic concentration and oxidation states of the different elements have been investigated using X-ray photoelectron spectroscopy (XPS). UV-visible absorption characterization confirmed the tunable optical properties of these materials. The proposed synthesis is scalable for commercial production with minimal environmental impact.

Published on 27 May 2010 on http://pubs.rsc.org | doi:10.1039/C001813A
Downloaded by City College of New York on 24 November 2010

Introduction

The last two decades have seen an exponential increase of reports on nanoparticles synthesis and their potential industrial applications.[1,2] The ability to produce high quality size tunable quantum dots using wet chemical approaches[3] contributed to this interest from both academia and industry. A variety of wet chemical synthesis routes have been developed, focusing mostly on the size distribution monodispersity, requiring extensive purification and size selection steps. Unfortunately the lack of scalability of these synthesis approaches and utilisation of large amount of organic solvents will continue to hinder their sustainable development and commercialisation. Development of simple, clean and effective nanoparticle synthesis routes[4,5] including the possibility of precursors separation and reuse[6] is critical to fulfil the potential of these nanoparticles.

Nanoparticles are used in numerous applications to address long term environmental and energy issues. Ultra-small metallic nanoparticles are used to improve gravimetric energy density of polymeric fuel cells.[7,8] Oxides nanomaterials are used to improve photocatalysis efficiency[9,10] and gravimetric energy density of lithium ion batteries.[11] Semiconductor nanoparticle are used to form 3D heterojunctions[12] and high density[13,14] photovoltaic films using non-vacuum coating techniques. These nanoparticles provide numerous advantages over bulk materials obtained *via* conventional vacuum deposition techniques. Nanoparticle-based coating techniques are inexpensive since they do not require high temperature and high vacuum processing. However, current fabrication processes of nanoparticles may have significant environmental impact that could negate these advantages. In recent years, numerous green chemistry approaches have been developed to synthesize nanoparticles to address this issue.[4,5,15] Often these synthesis processes have been developed to optimize utilization of bio-based precursors and to avoid organic solvents and toxic chemicals during the fabrication process. Several green techniques have been developed to produce transition metals and group II–VI semiconductor nanoparticles.[16] Other industrially relevant photovoltaic materials have received little attention. This is particularly the case of $Cu(In_{1-x}Ga_x)S_ySe_{1-y}$ (where x and y vary from 0 to 1 and 0 to 2 respectively), often refereed as CIGS. These CIGS materials, a promising alternative to silicon solar cells and other optoelectronic applications, are currently obtained using expensive and low yield co-evaporation bulk deposition techniques[17] and other particle-based techniques that are difficult to scale.[18–26]

Non-vacuum fabrication techniques of CIGS film from particles precursors is presently attracting great interest from both academia and industry. Both solid state and solution-based synthesis approaches have been used in the past to produce these particles. These synthesis techniques require numerous reagents, organic solvents and reaction steps at relatively high temperature with a significant amount of by-products. Reaction time, temperature, solvent and other preparation conditions are used to define the optimal synthesis process. Furthermore, obtaining small and monodispersed CIGS nanoparticles with tunable Ga content is very important for photovoltaic applications[17,27,28] and other potential applications.

Few attempts to synthesize $Cu(In_{1-x}Ga_x)S_2$ or $Cu(In_{1-x}Ga_x)Se_2$ nanoparticles have been reported. Even fewer attempts have been made to control the Ga content within the CIGS structure.[23–25] In their study, Ahn *et al.* used different organic solvents to prepare nanoparticle with size

[a]*Institute for Chemical Process and Environmental Technology National Research Council of Canada, 1200 Montreal Rd, Ottawa, ON, K1A 0R6, Canada. E-mail: farid.bensebaa@nrc.ca; Tel: +1-(613) 991-6347*
[b]*Chemistry Department, Science College, King Saud University, P.O.Box. 22452, Area code 11495, Riyadh, Saudi Arabia*

 This journal is © The Royal Society of Chemistry 2010

View Online

above 15 nm.[23] Using dichlorobenzene and relatively high synthesis temperature (180 °C), Panthani *et al.* succeeded in synthesizing CIGS nanoparticle with different Ga content.[25] These processes are hardly scalable with potentially significant negative environmental impact.[4]

Following our recent work,[14] we have used a microwave oven to synthesize CIGS nanoparticle with variable Ga content. Numerous studies have been published on applications of microwave heating for nanomaterials synthesis.[29] Low microwave processing[30–32] temperature (95 °C) for about half an hour is used. No organic solvent is used. Since selenium is already incorporated in these nanoparticles, no toxic H_2Se gas treatment is required for the synthesis of the final CIGS materials.

Experimental

$CuIn_{1-x}Ga_xSe_2$ nanoparticles with $x = 0$, 0.25 and 0.5 were prepared according to the following procedure. The value x corresponds to the relative percentage of Ga within the starting raw materials. Around 120 mg of copper acetate dihydrates was mixed with 300 ml de-ionized (DI) water in 500 mL round bottomed flask. Indium chloride ($InCl_3$) and Gallium chloride ($GaCl_3$) were added to the previous solution. Given the instability of the Ga precursor in the presence of oxygen, air exposure is minimised. Solution is degassed prior to Ga addition, and reaction was conducted under nitrogen atmosphere. The $GaCl_3$ and Na_2Se precursors were weighed in the glove box and kept under argon gas pressure. They were used immediately by diluting in water then added to the solution according to the description above. Except for Na_2Se obtained from Alfa-Aesar, all other chemicals were purchased from Sigma-Aldrich.

After stirring the Cu and In (with or without Ga) solution for two minutes, we added 2 mL from a fresh 6 mL solution consisting of 1 ml mercapto-acetic acid and 5 mL of de-ionized (DI) water. This new solution was stirred for 5 min, then disodium selenide (Na_2Se) was added. The color of solution turned to dark brown. The reaction vessel was transferred to the microwave oven (Mars 5X from CEM Corp. NC, equipped with a reflux condenser) and heated to about 95 °C for 30 min. After cooling, the solution product is centrifuged with DI water giving rise to a black powder.

After diluting the precipitate, a few drops of the resulting aqueous solution was deposited on a nickel grid and allowed to dry. TEM (transmission electron microscopy) analysis was recorded using a Philips CM20 200 kV electron microscope equipped with an Oxford Instruments energy dispersive X-ray diffraction detector. XRD characterization was performed at room temperature with Cu-Kα radiation using a Bruker diffractometer D8. Powder samples were uniformly spread over a low background silicon holder.

Results

Colloidal nanoparticles obtained following microwave heating and cleaning steps are characterized to provide information about size distribution, composition and structure. In this study, $CuIn_{1-x}Ga_xSe_2$ samples with the following values of the relative atomic concentration of Ga are synthesized and characterized: $x = 0$, 0.25 and 0.5.

Fig. 1 shows TEM images of as-synthesised $CuInSe_2$, $CuIn_{0.75}Ga_{0.25}Se_2$ and $CuIn_{0.5}Ga_{0.5}Se_2$ nanoparticles. In all cases sub-10 nm nanoparticles with relatively uniform size distribution are shown. The majority of the nanoparticles have an average size of about 4 nm in the case of $CuInSe_2$. Similar size distribution has been obtained elsewhere.[33] CIGS nanoparticles with higher Ga are slightly larger. It is also important to emphasize that no post-synthesis size selection has been performed. Indeed to obtain sub-10 nm nanoparticles, previous work used a large amount of different types of organic solvent to remove larger particle sizes.[33] This step is not only expensive and time consuming, but adds a negative environmental impact to the process. Furthermore, potentially significant reduction in the overall synthesis yield is expected, making these wet synthesis approaches quite prohibitive.

CIGS nanoparticle with higher Ga content showed relatively higher level of agglomeration. Presently, we can not explain why Ga-containing CIGS nanoparticles are more likely to agglomerate. Later, we will analyze the surface composition of these nanoparticles to detect any difference that could explain this trend.

Schulz *et al.* prepared sub-100 nm CIGS nanoparticles by reacting under nitrogen atmosphere a mixture of CuI, InI_3 and GaI_3 in pyridine with Na_2Se in methanol at low temperature.[13] The resulting nanoparticles are ill-defined with diameter size ranging from 10 to 30 nm. Using a similar approach, CIGS nanoparticles with a nominal chemical formulae of $Cu_{0.9}In_{0.64}Ga_{0.23}Se_2$ and average size of 20 nm have been also reported.[23,24] Panthani *et al.* reported CIGS nanoparticle with diameter size of 10–25 nm following a size selection step.[25] This size selection step requires a large volume of different organic solvents. A solvothermal process has been also used to synthesize CIGS nanoparticles using ethylenediamine as a solvent.[34] In this case, nanoparticles with a diameter in the range of 30–80 nm were obtained. Increasing heating temperatures up to 280 °C for more than 24 h using this solvothermal method give rise to larger particle size.[34]

In all these reports, organic solvents are used during the synthesis and also in cleaning and separation steps. Although relatively higher quality nanoparticles have previously been obtained, these organic solvents have negative environmental impact.

The average size distribution of CIGS nanoparticles obtained in this study is much lower than previously reported. Lower particle size distribution is important since they require lower temperature processing when dense films are prepared. Indeed, nanoparticle melting temperature is lowered when their diameter is reduced. The combination of uniform heating process using a microwave energy source and relatively lower processing temperature has lead to small and uniform CIGS nanoparticles. Microwave synthesis has been shown by this group to provide high quality Pt–Ru alloy nanoparticle with tunable properties.[30] Heating uniformity has been found to be a key attribute of microwave synthesis of metals,[30] oxides[31] and alloyed semiconductors[32] nanoparticles. However, current microwave design may need improvements to address potential hazards that may occur when implementing large scale productions.

To the best of our knowledge there is no report showing uniform sub-10 nm CIGS nanoparticles size distribution.

Published on 27 May 2010 on http://pubs.rsc.org | doi:10.1039/C001813A
Downloaded by City College of New York on 24 November 2010

View Online

Downloaded by City College of New York on 24 November 2010
Published on 27 May 2010 on http://pubs.rsc.org | doi:10.1039/C001813A

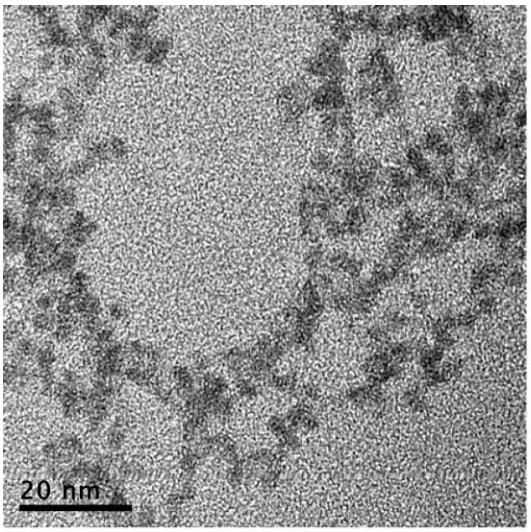

(a)

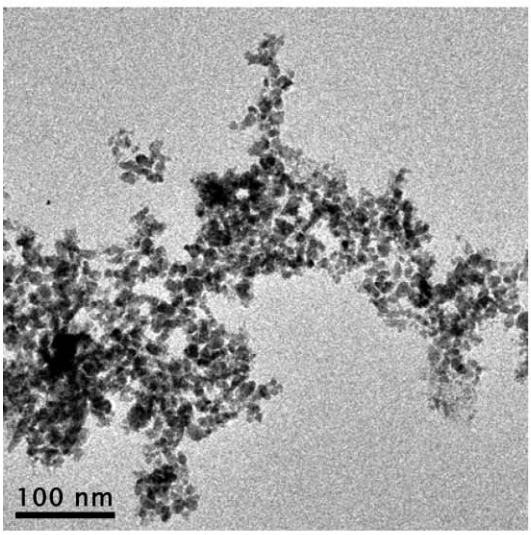

(b)

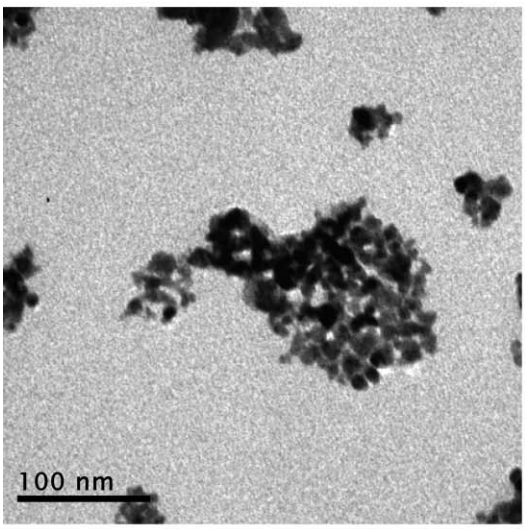

(c)

Fig. 1 TEM image of as synthesized: (a) $CuInSe_2$, (b) $CuIn_{0.75}Ga_{0.25}Se_2$ and (c) $CuIn_{0.5}Ga_{0.5}Se_2$ nanoparticles.

However, Castro *et al.* used chemical molecules containing Cu, In, S or Se to synthesize small sub-10 nm $CuInS_2$ and $CuInSe_2$ nanoparticles.[33] Besides using size-selective step to eliminate larger particles, their structure did not include gallium.

X-Ray diffraction (XRD) has been used to characterize the structure of these as-synthesized CIGS nanoparticles. Fig. 2 shows typical diffraction features of chalcopyrite materials. Three relatively broad diffraction peaks are detected around 28, 47 and 55°. These patterns are indicative of a chalcopyrite tetragonal structure after comparing with the Joint Committee on Powder Diffraction Standards (JCPDS) card File No. 27–0159. Indeed, these three peaks correspond to the (112), (220) and (116) planes of a tetragonal structure respectively.[27,28]

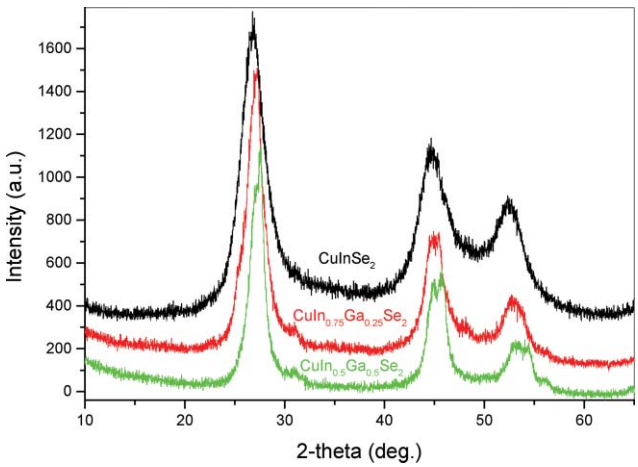

Fig. 2 XRD spectra of $CuInSe_2$ (black solid line), $CuIn_{0.75}Ga_{0.25}Se_2$ (red solid line) and $CuIn_{0.5}Ga_{0.5}Se_2$ (green solid line) nanoparticles.

The well-defined diffraction peak observed at $2\theta = 28°$ has been used to estimate the crystallite size of these nanoparticles. The signal-to-noise ratio of the XRD spectrum is the highest around this peak. Diffractions peak width of nanoparticles are much larger than those of bulk materials.[27,28] Line broadening of the XRD diffraction peaks has been used in the past to estimate the average crystallite size of nanoparticles. Peak broadening due to instrumental artefacts and strain are not considered here.

The size of the crystallites (d_c) has been determined using the Debye-Scherrer equation:[30,35]

$$d_c = 0.9\ \lambda/\beta\cos\theta$$

where β (in radians) is the linewidth at an angle 2θ (in radians) and λ is the X-ray wavelength, 1.5406 Å. Based on the linewidth of the (112) diffraction peak, we estimate the size of the crystallite to be around 3 nm. There is no significant variation in the peak linewidth using different Ga/In ratios. Thus the crystallite size does not change with Ga content.

A small but gradual peak shift is clearly observed for the (112) peak around $2\theta = 28°$ when Ga content is increased. Indeed, a difference of about 0.6 degree in the peak positions of $CuInSe_2$ and $CuIn_{0.5}Ga_{0.5}Se_2$ samples could be inferred from Fig. 2. This shift is assigned to a change in lattice dimensions. This trend is consistent with Vegard's law that support a gradual In–Ga alloying. This has been reported on bulk[27,28] and nanoparticle[25] based CIGS materials.

 This journal is © The Royal Society of Chemistry 2010

View Online

Published on 27 May 2010 on http://pubs.rsc.org | doi:10.1039/C001813A
Downloaded by City College of New York on 24 November 2010

Based on TEM and XRD data, we conclude that CIGS nanoparticles consist of single crystallite of 3 nm. The difference in diameter between XRD and TEM data could be assigned to a noncrystalline surface layer. Relatively larger CIGS nanoparticles with high Ga contents have been obtained. Indeed, an average diameter of about 4 nm or more has been estimated.

Displayed in Fig. 3 is the UV-absorption spectra of $CuInS_2$ nanoparticles (black dotted line), $CuInSe_2$ nanoparticle (black solid line), $CuIn_{0.75}Ga_{0.25}Se_2$ (red solid line) and $CuIn_{0.5}Ga_{0.5}Se_2$ (green solid line). For reference purpose, UV-visible absorption spectrum of water containing surfactant is included. Absorption peak around 975 nm is assigned to water since it is also observed on pure water. We could observe an increase in the onset of the absorption following this order: $CuInS_2$, $CuInSe_2$, $CuIn_{0.75}Ga_{0.25}Se_2$ and $CuIn_{0.5}Ga_{0.5}Se_2$. Similar UV-Visible absorption features are reported elsewhere on CIGS nanoparticle.[25,33–36] This could be explained by the increase in the bandgap when substituting sulfur by selenium and/or substituting indium by gallium.

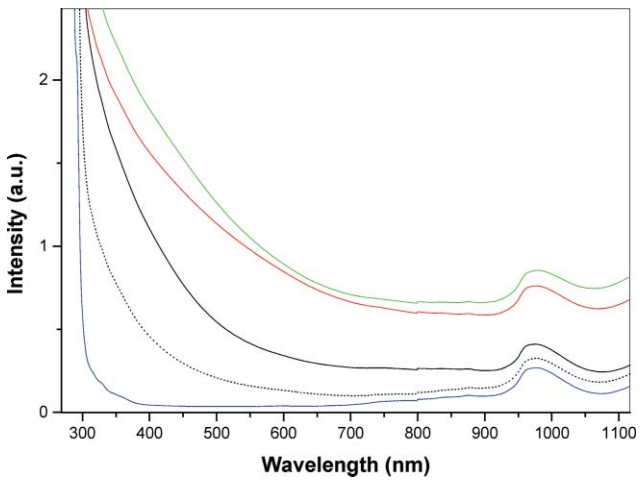

Fig. 3 UV-Visible absorption of aqueous solution (from bottom-to-top) of: acetic-acid (blue), $CuInS_2$ (black dotted line), $CuInSe_2$ (black solid line), $CuIn_{0.75}Ga_{0.25}Se_2$ (red solid line) and $CuIn_{0.5}Ga_{0.5}Se_2$ (green solid line) nanoparticles.

XPS is used to evaluate the oxidation states of the different elements within the CIGS nanoparticles and also characterize their surface composition. Survey XPS scans showed the presence of elements such as Cu, In, Ga and Se. Some differences in the relative ratios are noticed from sample to samples. Other elements such as C and O have been also observed. The presence of these elements is assigned to the surfactant and contaminations on the surface of the nanoparticle. Although relatively high amount of mercapto-acetic acid is used, the final product does not contain significant amount of surfactant following cleaning steps. Indeed we didn't observe any dominant Sulfur peak using XPS. In solid-state, these nanoparticle tend to agglomerate following surfactant removal. Adventitious carbon on the surface of these nanoparticles is also believed to contribute significantly to the overall XPS signal. Note that redispersion of nanoparticles in aqueous solution requires the addition of surfactant followed by stirring.

High-resolution XPS data showed the presence of single $Cu2p_{3/2}$ centered around 932.0 eV. This position is consistent with a chalcopyrite structure.[37,38] Indeed $Cu2p_{3/2}$ peaks from $CuInSe_2$ and Cu_2Se with assigned positions around 931.9 and 932.8 eV respectively have been reported.[38]

Table 1 Summary of relative atomic concentrations obtained by XPS for three CIGS samples

	$CuInSe_2$	$CuIn_{0.75}Ga_{0.25}Se_2$	$CuIn_{0.5}Ga_{0.5}Se_2$
Ga	0	0.7	1.29
Cu	8.36	9.65	10.86
O	21.8	20.16	17.31
In	12.21	11.18	8.07
C	42.52	41.8	45.04
Se	15.11	16.51	17.43

In the case of $Se3d_{5/2}$, optimal curve fitting indicates the presence of two distinct peaks at around 54.2 and 55.2 eV. These two peaks are assigned to Se^0 and Se^{-2} species respectively. This assignment is consistent with high resolution XPS of bulk CIGS film reported in the literature.[39] It is difficult to determine the origin of these two selenium states based solely on XPS data. We could however speculate the coexistence of two structures containing metallic and reduced selenium.

Relative atomic concentrations of these CIGS samples within the probing depth of XPS are summarized in Table 1. Carbon and oxygen are assigned to the surfactant and adventitious carbon contaminations at the surface of the nanoparticles. Values of Cu/Se ratio are estimated to be 0.55, 0.58 and 0.62 for $CuInSe_2$, $CuIn_{0.75}Ga_{0.25}Se_2$ and $CuIn_{0.5}Ga_{0.5}$ respectively. It seems that there is nearly no significant change in the value of Cu/Se for the different x values. This is consistent with XRD data that do not show any peak related to poor Cu CIGS materials diffraction characteristics.[14]

Cu/(In+Ga) ratio of 0.68, 0.81 and 1.16 have been estimated for $CuInSe_2$, $CuIn_{0.75}Ga_{0.25}Se_2$ and $CuIn_{0.5}Ga_{0.5}Se_2$ respectively. The trend of increased Cu/(In+Ga) as the relative amount of Ga is increased is difficult to explain. It is however possible that there is a small excess of copper rich phase at the surface of nanoparticle. Another possible explanation is the relative increase in agglomeration when Ga content is increased. Indeed TEM micrographs indicate that Ga-rich CIGS nanoparticles are agglomerated. With larger particles, copper segregation at the surface when Ga content is increased will give rise to relatively higher XPS copper signal. This is does not contradict XRD data showing a single phase on all CIGS materials. Indeed, XPS is a surface sensitive technique which is not the case of XRD.

Work is under way to replace mercapto-acetic acid surfactant with other water soluble bio-based alternatives. It will be also of interest to study the effect of other parameters such as reagents compositions and concentrations on the nanoparticles properties.

Conclusions

For the first time CIGS nanoparticle with an average size of 4 nm and variable Ga content has been synthesized without using organic solvent. These nanoparticles are stable in aqueous solution for several weeks. Size-selective step often used for quantum dot synthesis is not performed in this work. XRD data clearly showed change in lattice constant when Ga content is increased. UV-Visible data confirmed tunability of the optical

View Online

properties. Proposed synthesis approach will thus have minimal negative environmental impact since even spent water solvent could be easily recycled. Except for the surfactant, proposed synthesis satisfies the green chemistry principles. These sub-10 nm nanoparticles could be integrated in the fabrication of high density CIGS photovoltaic films and other optoelectronic applications.

References

1 *Nanoparticles: From Theory to Application*, ed. G. Schmid, Wiley-VCH, Weinheim, 2004.
2 H. Fukumori and H. Ichikawa, *Adv. Powder Technol.*, 2006, **17**, 1–28.
3 C. B. Murray, D. J. Norris and M. G. Bawendi, *J. Am. Chem. Soc.*, 1993, **115**, 8706–8717.
4 J. A. Dahl, B. L. S. Maddux and J. E. Hutchison, *Chem. Rev.*, 2007, **107**, 2228–2269.
5 K. N. Thakkar, S. S. Mhatre and R. Y. Parikh, *Nanomed.: Nanotechnol., Biol. Med.*, 2010, **6**, 257, and references therein.
6 P. T. Anastas and J. C. Warner, *Green Chemistry: Theory and Practice*, Oxford University, Oxford, 1998.
7 N. M. Markovic and P. N. Ross, *Catal. Technol.*, 2000, **4**, 110–126.
8 F. Bensebaa, A. A. Farah, D. Wang, C. Bock, X. Du, J. Kung and Y. LePage, *J. Phys. Chem. B*, 2005, **109**, 15339.
9 B. L. Abrams and J. P. Wilcoxon, *Crit. Rev. Solid State Mat. Sci.*, 2005, **30**, 153–182.
10 A. Hagfeldtt and M. Gratzel, *Chem. Rev.*, 1995, **95**, 49–68.
11 D. R. Rolison, J. W. Long, J. C. Lytle, A. E. Fischer, C. P. Rhodes, T. M. McEvoy, M. E. Bourg and A. M. Lubers, *Chem. Soc. Rev.*, 2009, **38**, 226–252.
12 W. U. Huynh, J. J. Dittmer and A. P. Alivisatos, *Science*, 2002, **295**, 2425–2427.
13 D. L. Schulz, C. J. Curtis, R. A. Flitton, H. Weisner, J. Keane, R. J. Matson, K. M. Jones, P. A. Parilla, R. Noufi and D. S. Ginley, *J. Electron. Mater.*, 1998, **27**, 433–437.
14 F. Bensebaa, C. Durand, A. Aouadou, L. Scoles, X. Du, D. Wang and Y. Le Page, *J. Nanopart. Res.*, 2009, DOI: 10.1007/s11051-009-9752-5.
15 Y. Mao, T. J. Park, F. Zhang, H. Zhou and S. S. Wong, *Small*, 2007, **3**, 1122.
16 H. Zhang, D. Wang, B. Yang and H. Mohwald, *J. Am. Chem. Soc.*, 2006, **128**, 10171–10180.
17 I. Repins, M. J. Contreras, E. B. Romero, C. DeHart, J. Scharf, C. L. Perkins and R. Noufi, *Progr. Photovolt.: Res. Appl.*, 2008, **16**, 235–239.
18 B. M. Basol, *Thin Solid Films*, 2000, **361–362**, 514–519.
19 V. K. Kapur, A. Bansal and O. L. Asensio, *Thin Solid Films*, 2003, **431–432**, 53–57.
20 C. Eberspacher, C. Frederic, K. Pauls and J. Serra, *Thin Solid Films*, 2001, **387**, 18–22.
21 M. Kaelin, D. Rudmann, F. Kurdesau, T. Meyer, H. Zogg and A. N. Tiwari, *Thin Solid Films*, 2003, **431–432**, 58–62.
22 M. Kaelin, D. Rudmann, F. Kurdesau, T. Meyer, H. Zogg and A. N. Tiwari, *Thin Solid Films*, 2005, **480–481**, 486–490.
23 S. J. Ahn, K. H. Kim and K. H. Yoon, *Colloids Surf., A*, 2008, **313–314**, 171–174.
24 S. J. Ahn, K. H. Kim, Y. G. Chun and K. H. Yoon, *Thin Solid Films*, 2007, **515**, 4036–4040.
25 M. G. Panthani, V. Akhavan, B. Goodfellow, J. P. Schmidtke, L. Dunn, A. Dodabalapur, P. F. Barbara and B. A. Korgel, *J. Am. Chem. Soc.*, 2008, **130**, 16770–16777.
26 C. J. Carmalt, D. E. Morrison and I. P. Parkin, *J. Mater. Chem.*, 1998, **8**, 2209–2211.
27 V. Alberts, *Mater. Sci. Eng., B*, 2004, **107**, 139–147.
28 V. Alberts, *Thin Solid Films*, 2009, **517**, 2115–2120.
29 G. A. Tompsett, W. C. Conner and K. S. Yngvesson, *ChemPhysChem*, 2006, **7**, 296–319, and references therein.
30 F. Bensebaa, N. Patrito, Y. Le Page, P. L'Ecuyer and D. Wang, *J. Mater. Chem.*, 2004, **14**, 3378–3384.
31 F. Bensebaa, F. Zavaliche, P. L'Ecuyer, R. W. Cochrane and T. Veres, *J. Colloid Interface Sci.*, 2004, **277**, 104–110.
32 V. Firth, Y. Tao, D. Wang, J. Ding and F. Bensebaa, *J. Mater. Chem.*, 2005, **15**, 4367–4372.
33 S. L. Castro, S. G. Bailey, R. P. Raffaelle, K. K. Banger and A. F. Hepp, *J. Phys. Chem. B*, 2004, **108**, 12429–12435.
34 Y. G. Chun, K. H. Kim and K. H. Yoon, *Thin Solid Films*, 2005, **480–481**, 46–49.
35 C. Czekelius, M. Hilgendorf, L. Spanhel, I. Bedja, M. Lerch, G. Muller, U. Bloeck, D. S. Su and M. Gersig, *Adv. Mater.*, 1999, **11**, 643–646.
36 J. J. Nairn, P. J. Shapiro, B. Twamley, T. Pounds, R. von Wandruszka R, T. R. Fletcher, M. Williams, C. Wang and M. G. Norton, *Nano Lett.*, 2006, **6**, 1218–1223.
37 J. Llanos, A. Buljan, C. Mujica and T. J. Ramirez, *J. Alloys Compd.*, 1996, **234**, 40–42.
38 E. P. Domashevskayaa, V. V. Gorbachev, V. A. Terekhova, V. m. Kashkarova, E. V. Panfilova and A. V. Shchukarev, *J. Electron Spectrosc. Relat. Phenom.*, 2001, **114–116**, 901–908.
39 B. Canava, J. Vigneron, A. Etcheberry, J. F. Guillemoles and D. Lincot, *Appl. Surf. Sci.*, 2002, **202**, 8–14.

Downloaded by City College of New York on 24 November 2010
Published on 27 May 2010 on http://pubs.rsc.org | doi:10.1039/C001813A

 This journal is © The Royal Society of Chemistry 2010